Microwave High-Resolution 3D SAR Imaging of Corroded Reinforcing Steel Bars in Mortar Subjected to Accelerated Electrochemical Corrosion

C. Liu[1], S. Barker[1], L. Fan[2], M.T. Ghasr[1], G. Chen[2] and R. Zoughi[1]

[1]*Applied Microwave Nondestructive Testing Laboratory (amntl)*
Electrical and Computer Engineering Department
Missouri University of Science and Technology (S&T)
Rolla, MO, USA, Email: cl2b5@mst.edu

[2]*Civil, Architectural and Environmental Engineering Department*
Missouri University of Science and Technology (S&T)
Rolla, MO, USA

Abstract

Corrosion of reinforcing steel bars (rebars) embedded in concrete is a significant maintenance, rehabilitation and safety issue as it relates to the overall health of concrete structures, particularly those subjected to cyclical chloride attack. Over the years several inspection methods have been used to detect and assess this corrosion with limited success. Wideband microwave imaging, using synthetic aperture radar (SAR) techniques, has shown great potential for producing 3D images of structures containing rebars. Although these investigations have shown great promise, a methodical approach to investigate the overall efficacy of this imaging technique has not yet taken place. Steel corrosion byproduct (i.e., rust) is a relatively high permittivity and high loss dielectric material. Relatively high loss factor results in the absorption of the irradiating microwave energy, leading to rebar image becoming less prominent. Hence, high-resolution images of concrete samples subjected to accelerated corrosion are expected to result in a better understanding and limitations of this imaging approach. This paper outlines the results of an ongoing investigation using wideband microwave 3D SAR imaging technique applied to mortar samples with rebars that were cyclically corroded using an accelerated corrosion process. Simulation results show the presence corrosion on rebars can be clearly detected through attenuations of microwave signal. Measurements as a function of mortar water-to-cement (*w/c*) ratio and corrosion condition are also conducted. Discussion of similarities and differences between the simulation and experimental results are also provided.

1. Introduction

It is commonly known that corrosion of embedded steel bars (rebars) in concrete members, due to chloride attack, is a major concern with respect to the health and maintenance of civil infrastructures such as roadways, bridges and dams (Koch, *et al.,* 2001). Corrosion byproducts (i.e., rust) occupy a larger volume than the materials that produced it, leading to stresses that ultimately cause cracking and spalling in these structures. Consequently, it is critical to devise a robust detection and evaluation techniques to monitor degradation of these structures due to

rebar corrosion. Theoretical modeling results predicting corrosion rates are not always corroborated by experimental verifications as pointed out by (ACI 228.2R, 1998) and (Poursaee, *et al.,* 2007), and there exists significant discrepancies in accuracy associated with different testing methods (Flis, *et al.,* 1993). For studying the effect of corrosion, electrochemical testing technique is a method of inducing corrosion on an embedded rebar with reasonable control of the corrosion growing process (Malhotra and Carino, 2004; Poursaee, *et al.,* 2011). This process can then be combined with different testing techniques to evaluate their efficacy for detecting and assessment of corrosion level.

Clearly, a robust and accurate nondestructive testing (NDT) approach for assessing steel rebar condition is highly desirable. To this end, high-resolution microwave synthetic aperture radar (SAR) imaging technique has shown great potential for this purpose in recent years (Kharkovsky, *et al.,* 2011; Ghasr, *et al.,* 2015). However, this technique also has certain limitations which need to be considered when using for rebar corrosion assessment. At microwave frequencies concrete is a lossy and inhomogeneous material (i.e., presence of aggregates). Therefore, a microwave signal interacting with the internal structures of a concrete structure undergoes significant attenuation and scattering, as a function of the operating frequency (i.e., wavelength). Lower microwave frequencies penetrate deeper into concrete and are less affected by the scattering influences of the aggregates. However, lower frequencies produce images with coarser spatial and depth resolutions, leading to images that may not be as clearly indicative of corrosion in rebars (Ghasr, *et al*., 2015). In this paper, we investigate the effect of cyclically corroding rebars using an accelerated corrosion process, in mortar samples, while performing electromagnetic simulations as well as SAR imaging experiments.

2. Electromagnetic Simulations

Electromagnetic simulations were performed to investigate the theoretical capabilities of SAR imaging for detecting and assessing corrosion level in rebras embedded in mortar. Figure 1 shows the simulation schematic where a plane-wave, at J-band (5.85-8.2 GHz), impinges upon a mortar sample (cross-section shown) with two embedded rebars, one of which (on the right) has varying thicknesses of corrosion on it (discrete 5% increase).

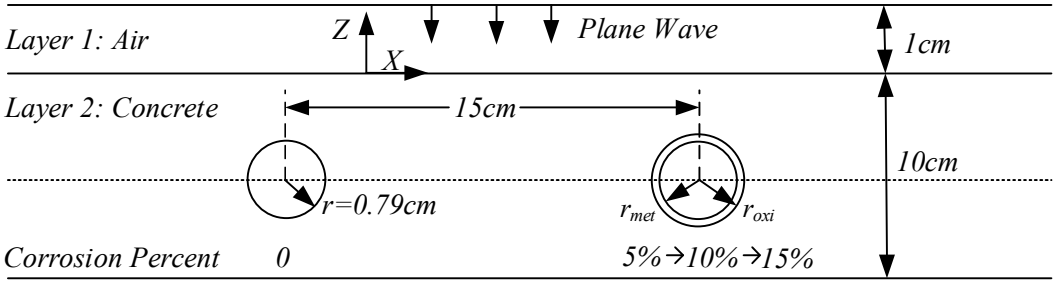

Figure 1: Electromagnetic simulation configuration for a mortar sample with embedded rebars.

The dielectric constant of the sample was taken to be ($\varepsilon_r = 4\text{-}j0.2$), while the corrosion byproduct (i.e., rust) dielectric constant was taken to be ($\varepsilon_r = 12.5\text{-}j2.6$) (Fallahpour, *et al.,* 2014). Using CST Microwave Studio®, the reflection coefficient measured at the location of the

incident wave (1 cm above the sample) was calculated along the sample (from right to left). This data, representing the measured reflection coefficient, was then passed through the Green's function-based SAR algorithm (Fallahpour, *et al*., 2014) to produce an image of the cross-section of the sample. The two embedded steel bars are placed at the same depth of 150 cm within the sample, and 15 cm apart, which is large compared with the operating wavelength, to ensure minimal interactions between the two. The thickness of corrosion layer, r_{oxi}, was calculated according to:

$$r_{met} = r\sqrt{1-N_c}\ ,\ r_{oxi} = r\sqrt{1+3N_c} \qquad (1)$$

where, r_{met} is the radius of rebar, and N_c is the ratio of corrosion (lost mass of a rebar due to corrosion over its original mass). No corrosion was considered on the left rebar while only the one on the right was corroded as a function of increasing corrosion percentage, N_c, from 0% to 5%, 10% and 15%. The calculated thicknesses are shown in Table 1.

Table 1: Size of differently-corroded rebars.

Corrosion Percentage	r_{met} (cm)	r_{oxi} (cm)	Thickness (r_{oxi}-r_{met}) (cm)
5%	0.770	0.847	0.077
10%	0.749	0.900	0.151
15%	0.728	0.951	0.223

Figure 2a-d show the results of these simulations, in the form of cross-section images of the sample with varying percentage of corrosion. The results clearly show the effect of increasing corrosion level in the (right) rebar image intensities, as a direct result of the lossy nature of the dielectric constant of corrosion/rust. In addition, the results show that the decrease in the image intensity is not a linear function of increasing corrosion level.

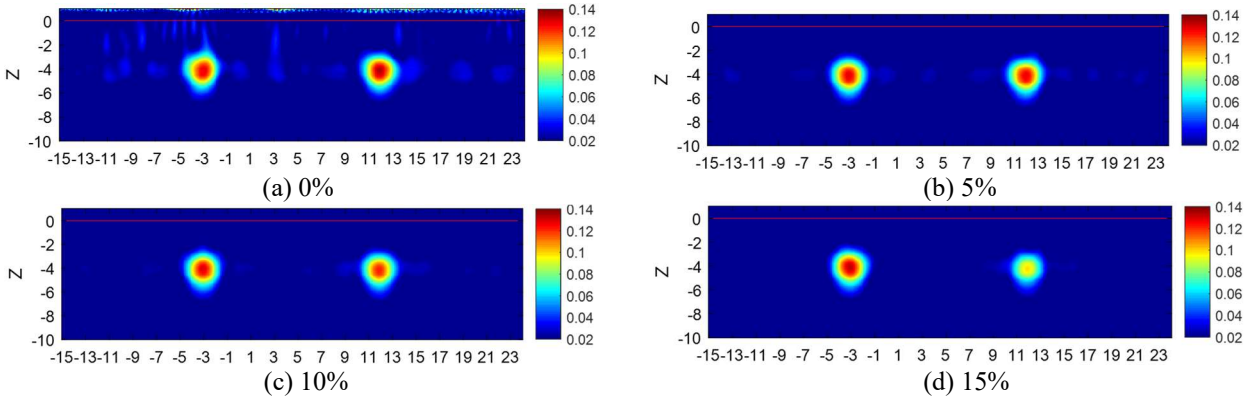

Figure 2: Simulation results for: a) 0%, b) 5%, c) 10% and d) 15% corrosion (N_c), respectively.

To more quantitatively show the effect of increasing corrosion level on the rebar on the right, image intensity magnitude at x = 12 cm, which correspond to the center position of the right rebar in the x-direction (from left to right) is extracted and shown in Figure 3. The result shows the gradual, yet non-linear change in the image intensity. More importantly, the non-linear changes of green function in terms of propagation distance (Mosig and Melcon, 2003) leads to the quick decay of signals from 10% case to 15% case while small portion from 0% to 10%.

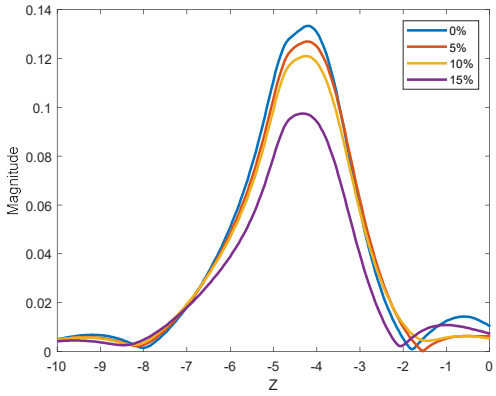

Figure 3: Image intensity from the right rebar as a function of increasing corrosion level.

It is important to note that this simulation is preliminary and does not take into account the ribs in the rebar and the effect of their corrosion process and henceforth on the microwave signal scattering; permeation of corrosion byproduct in the mortar material around the rebar; cracking of mortar around the rebar; etc. Further investigation into this complex issue will be ongoing.

3. Mortar Samples and Experimental Cyclical Corrosion Procedure

To investigate the capabilities of the SAR imaging technique for detecting cyclically-corroded rebars, two sets of mortar samples, M1 and M2, with water-to-cement ratios (*w/c*) of 0.55 and 0.40 were cast, with three reinforcing steel bars embedded in each. The mix proportions of the mortars are shown in Table 2. After casting, the specimens were covered with wet burlap and plastic sheet to prevent surface cracking due to drying shrinkage. The specimens were demolded after 24 hours, and then cured in an environmental chamber for 28 days. Subsequently, they were placed in a temperature-controlled room, at 70°C and for approximately 20 days, to remove any excess moisture. Figure 4 shows pictures of the form with three rebars and the cast sample, respectively. Dimensions of the final mortar are 42.5 cm (L), 26.5 cm (W) and 12 cm (H). The mortar cover thickness is 5 cm and the rebars are one-foot long with a dimeter of 1.91 cm.

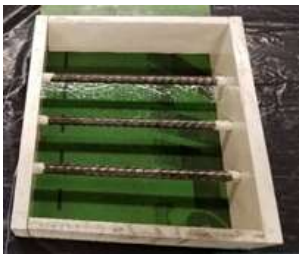

Table 2: Mix proportions of the two mortar mixtures.

Types of mortar	M1	M2
Water	0.55	0.4
Ordinary Portland cement	1.0	1.0
Missouri river sand	2.81	1.83

Figure 4: Pictures of casting frame (left), one of the samples (middle), and mix proportions (right).

For the cyclical procedure of corroding the rebars, each sample was placed in a saltwater (NaCl solution) bath with a salinity of 3.5% (by wt.). The saltwater level was kept 0.5 cm lower than the lower edge of steel bars in order to avoid electrical short-circuit between the extruded steel rod and the saltwater solution. Then, a constant current of 500 $\mu A/cm^2$ was impressed through the rebars on both sides to accelerate corrosion until the mass loss of the steel bar reached 0.1%. No current was passed through the middle rebar. In this way, the middle rebar image could be

used as a reference with which to compare the other two rebar images. Subsequent to each soaking cycle, the sample was removed and placed in the temperature-controlled room to remove the excess water. Each day the mass of the sample was measured until such time there was no appreciable change in the mass. Subsequently, SAR images from both sides of the sample were produced at J-band (5.85-8.2 GHz) and X-band (8.2-12.4 GHz), respectively. The penetration of the microwave signal is higher at the former frequency band than the latter. However, the X-band images were produced for comparison purposes. The flow-chart of the entire experimental process is illustrated in Figure 5.

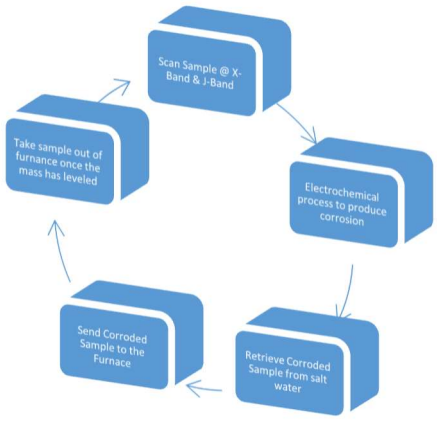

Figure 5: Flow-chart of the cyclical electrochemical corrosion and scanning procedure.

4. Experimental Results

Images at J-band (5.85-8.2 GHz) obtained by scanning the top side of the mortar sample with 0.55 water-to-cement ratio (*w/c*) are shown in Figure 6, subsequent to the third soaking cycle. Result of vertical cross section (perpendicular to rebars) is given by the left image and is taken from the middle position of the rebar, x= 132.5 mm, while the horizontal cross-section image on the right corresponds to an image slice at the plane ~6.5 cm below the top surface, approximately corresponding to the depth of the rebars. Both images clearly display the embedded three rebars. However, the difference between the two corroded rebars and the middle non-corrosion rebar is not very apparent. We believe the reason for this is the fact that the thickness of corrosion is still insignificant after 21 hours of electrochemical process, which is estimated to be only ~14 μm. Algorithm about detecting different corrosion levels based on the obtained SAR image data is currently being developed, and will be applied to these and subsequent images.

5. Conclusions

Microwave SAR imaging technique has the potential for being an efficient method for detecting corroded embedded steel bars in cementitious materials. Electromagnetic simulations on a mortar sample with two rebars with different levels of corrosion were performed, along with experiments involving cyclically corroding the rebars using an electrochemical process. Both simulated and experimental results showed that corroded rebars can be distinguished from non-corroded rebars. Cyclical corrosion will continue and further experimental results will be reported later.

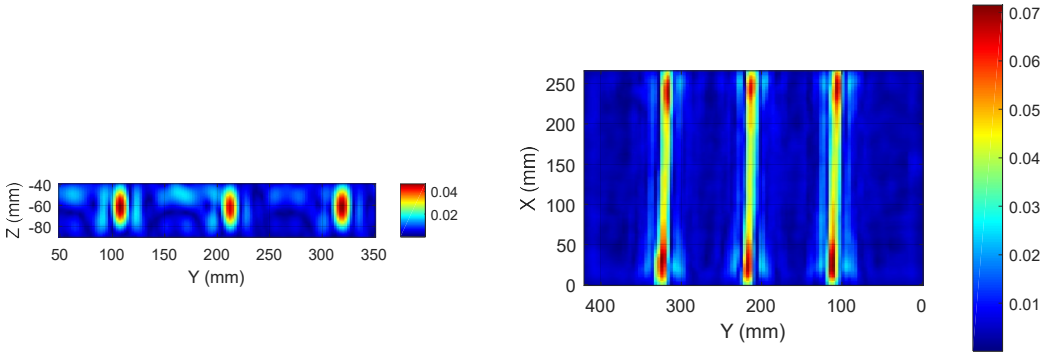

Figure 6: 2D microwave images in two cross-sections, vertical (left) and horizontal (right).

References

ACI Committee 228, "Nondestructive Test Methods for Evaluation of Concrete in Structures (ACI 228.2R-98), *American Concrete Institute*, Farmington Hills, MI, p. 62, 1998 (Reapproved 2004).

Fallahpour, M., Case, J. T., Ghasr, M.T., and Zoughi, R., "Piecewise and Wiener filter-based SAR techniques for monostatic microwave imaging of layered structures," *IEEE Transactions Antennas Propagation*, vol. 62, no. 1, pp. 282–294, 2014.

Flis, J., Sabol, S., Pickering, H., Seghal, A.; Osseo-Asare, K., and Cady, P., "Electrochemical Measurements on Concrete Bridges for Evaluation of Reinforcement Corrosion Rates," *Corrosion*, V. 49, No. 7, pp. 601-613, 1993.

Ghasr, M.T., Y. LePape, D.B. Scott, and R. Zoughi, "Holographical Microwave Imaging of Corroded Steel Bars in Concrete," *American Concrete Institute (ACI) Materials Journal*, vol. 112, no. 1, pp. 115-124, January 2015.

Kharkovsky, S., Case, J.T., Ghasr, M.T.; Zoughi, R., Bae, S.W., and Belarbi, A., "Application of Microwave 3D SAR Imaging Techniques for Evaluation of Corrosion in Steel Rebars Embedded in Cement-Based Structures," *Review of Progress in Quantitative Nondestructive Evaluation* V. 31B, Burlington, VT, July 17-22, V. 1430, AIP Conference Proceedings, D. O. Thompson and D. E. Chimenti, eds., American Institute of Physics, Melville, NY, pp. 1516-1523, 2011.

Koch, G.H., Brongers, M.P.H., Thompson, N.G., Virmani, Y.P., and Payer, J.H., "Corrosion Costs and Preventive Strategies in the United States," Report FHWA-RD-01-156, report by CC Technologies Laboratories, Inc. to Federal Highway Administration (FHWA), Office of Infrastructure Research and Development, p. 784, 2001.

Malhotra, V.M., and Carino, N.J., Handbook on Nondestructive Testing of Concrete, second edition, CRC Press, Boca Raton, FL, 2004.

Poursaee, A., "An Analysis of the Factors Influencing Electrochemical Measurements of the Condition of Reinforcing Steel in Concrete Structures," *Ph.D. Thesis, University of Waterloo*, Waterloo, ON, Canada, p. 298, 2007.

Poursaee, A., "Corrosion Measurement Techniques in Steel Reinforced Concrete," *Journal of ASTM International*, vol. 8, no. 5, pp. 1-15, 2011.

Mosig, J.R., Melcon, A.A., "Green's functions in lossy layered media: integration along the imaginary axis and asymptotic behavior," *IEEE Transactions Antennas Propagation.*, vol. 51, pp. 3200–3208, 2003.